Journal of Materials Chemistry B

PAPER

View Article Online
View Journal | View Issue

Cite this: J. Mater. Chem. B, 2019, 7, 6994

Bioreducible and acid-labile polydiethylenetriamines with sequential degradability for efficient transgelin-2 siRNA delivery†

Pengchong Wang,‡[a] Yan Yan,‡[a] Ying Sun,[a] Rui Zhang,[a] Chuanchuan Huo,[a] Lu Li,[b] Ke Wang,[a] Yalin Dong *[c] and Jianfeng Xing *[a]

Received 13th June 2019,
Accepted 1st October 2019

DOI: 10.1039/c9tb01183h

rsc.li/materials-b

The transgelin-2 (TAGLN2) protein plays an important role in multidrug resistance in human breast cancer. siRNA mediated gene silencing of TAGLN2 is a promising strategy for paclitaxel resistance reversal in breast cancer. In this study, a series of bioreducible and acid-labile polydiethylenetriamines (PDs) with different proportions of cross-linkers were synthesized. TAGLN2 siRNA was condensed by PDs to form dual-responsive nanocomplexes, and these nanocomplexes were hypothesized to partially degrade in the acidic environment of endosomes, and then completely degrade in the reducing environment of the cytoplasm to release siRNA. It was found that PDs have good water solubility, acid–base buffering capacity, suitable degradability and high biocompatibility. Moreover, PDCKM can deliver TAGLN2 siRNA into MCF-7/PTX cells and inhibit the expression of TAGLN2 even better than PEI 25k. Besides, paclitaxel showed higher cytotoxicity in cells incubated with PDCKM/TAGLN2 siRNA nanocomplexes. These results suggested that PDs have great potential for safe and efficient siRNA delivery to reverse paclitaxel resistance in breast cancer.

Introduction

Breast cancer is a very common type of cancer in women. Paclitaxel (PTX) represents one of the most predominant chemotherapeutic agents and is still an important medication for breast cancer therapy.[1] However, multidrug resistance (MDR) in tumor cells has become a major obstacle for effective breast cancer therapy.[2] There are many mechanisms involved in multidrug resistance in tumor cells, including the over expression of the ATP-binding cassette (ABC) transporter superfamily, such as P-glycoprotein (P-gp) and multidrug resistance-associated protein (MRP), the increase of level of glutathione-dependent detoxification enzyme system, apoptosis inhibition in tumor cells and some new molecular markers of multidrug resistance. It has been reported that Transgelin-2 (TAGLN2), an actin cross-linking/gelling protein that is involved in calcium interactions and regulates contractile properties, was highly expressed in the paclitaxel resistant human breast cancer (MCF-7/PTX) cell line. It could regulate the expression of the ABC transporter and played an important role in invasion metastasis and paclitaxel resistance in human breast cancer.[3–5]

RNA interference (RNAi), that mediates gene silencing and down-regulates the expression of proteins by small interfering RNA (siRNA), is a promising strategy for the reversal of multidrug resistance and the treatment of breast cancer. Zheng *et al.* found that the sensitivity of MCF-7/PTX cells to paclitaxel and some other chemotherapy drugs increased after knockdown of TAGLN2 by siRNA. Moreover, the mRNA and protein levels of BCRP, MDR1 and MRP1 expression were significantly reduced following down-regulation of TAGLN2.[6] These results indicated the potential of TAGLN2 siRNA to reverse multidrug resistance in breast cancer. However, it is a major stumbling block for safe and efficient delivery of siRNA to the target tumor site. Although some non-viral vectors including liposomes, micelles, cationic polymers, dendrimers and nanoparticles were developed as siRNA carriers, their severe cytotoxicity, low transfection efficiency and poor selectivity greatly restrict their clinical applications in breast cancer.[7–9]

Cationic polymers, such as polyethyleneimine (PEI),[10,11] chitosan (CS), poly(amide amine) (PAMAM),[12] poly(β-amino ester) (PAE)[13,14] and poly-L-lysine (PLL), with the ability to bind

[a] School of Pharmacy, Xi'an Jiaotong University, 76 Yanta West Road, Xi'an 710061, Shaanxi, China. E-mail: xajdxjf@mail.xjtu.edu.cn; Fax: +86-29-82655139; Tel: +86-29-82655139
[b] Laboratory Animal Center, Health Science Center of Xi'an Jiaotong University, Xi'an, Shaanxi, China
[c] Department of Pharmacy, The First Affiliated Hospital of Xi'an Jiaotong University, Xi'an, Shaanxi, China. E-mail: dongyalin@mail.xjtu.edu.cn; Fax: +86-29-85323240; Tel: +86-29-85323241

† Electronic supplementary information (ESI) available. See DOI: 10.1039/c9tb01183h

‡ These authors contributed equally to this work.

and condense siRNA into compact complexes, can efficiently protect the nucleic acid from degradation mediated by enzymes and facilitate cellular uptake. These nanocomplexes will be limited in endosomes which have a lower pH (5.5–6.5) than physiological pH (7.4) after entering the cell. As time goes on, the endosomes fuse with lysosomes, and the acidic pH (4.5–5.5) and enzymes result in the degradation of siRNA.[15,16] Some cationic polymers show strong buffering capacity in the pH range from 5.0 to 7.4, and this property leads to a phenomenon known as the ''proton sponge effect''. Protonated amines of the polymers lead to endosomal swelling and lysis, and cause the nanocomplexes to escape from the endosomes and release into the cytoplasm to silence gene expression.[17,18] It has been well-established that, the cationic polymers with high molecular weight (M_w) have a higher positive charge density and improved transfection efficiency.[19,20] At the same time, high M_w cationic polymers have severe cytotoxicity. The compact structure of the nanocomplexes decreases the siRNA release in cells and the poor selectivity toward the tumor site brings serious side effects.[21–24] For these reasons, it is high time to develop biodegradable cationic polymers with good biocompatibility, high transfection efficiency, good selectivity and tumor targeting ability.

A successful strategy to prepare favorable siRNA carriers is to introduce degradable bonds into the polymer backbone, such as disulfide bonds, ketal bonds and hydrazone bonds.[25–27] As previously reported, disulfide bonds will be cleaved in an intracellular environment in which the concentration of reduced glutathione (GSH) and thioredoxin reductase is much higher than that in the extracellular matrix. This degradation triggers the fast release of siRNA from the nanocomplexes and improves the transfection efficiency.[28,29] It is demonstrated that acid-labile cationic polymers will be degraded into monomers or lower M_w polymers in the acidic environment of endosomes.[30,31] An enormous number of small molecular products advantageously increase the osmotic pressure of endosomes and contribute to endosomal disruption and endosomal escape.[26] In this study, therefore, cationic PDs with disulfide bonds and ketal bonds were developed as TAGLN2 siRNA carriers. Diethylenetriamine (DETA) was polymerized using *N*,*N*′-methylenebisacrylamide (MBA), *N*,*N*′-cystamine bisacrylamide (CBA) and ketal containing diacrylate (KDA) as cross-linkers to prepare a series of bioreducible and acid-labile branched PDs. It was hypothesized that PDs can condense siRNA into nanocomplexes and passively target tumor tissue through the enhanced permeation and retention (EPR) effect.[32–34] The positive surface charges of the nanocomplexes enhance tumor cell uptake through electrostatic interaction with the negative charges of the cytomembrane.[35] After tumor cell uptake, the bioreducible and acid-labile PDs partially degrade in the acidic environment of endosomes and increase the osmotic pressure of endosomes, leading to endosomal disruption and endosomal escape. GSH is highly expressed in the cytoplasm of tumor cells, but low in endosomes, so that disulfide bonds will remain intact in endosomes. After this, nanocomplexes were released into the cytoplasm, and then disulfide bonds were cleaved in the reduction environment of the tumor cytoplasm; PDs were completely degraded and siRNA can be released from the nanocomplexes rapidly to suppress gene expression (shown in Scheme 1). Based on these properties, we anticipate that bioreducible and acid-labile PDs can sequentially degrade in the endosome and the cytoplasm, and are available to deliver TAGLN2 siRNA into MCF-7/PTX cells to reverse paclitaxel resistance.

Materials and methods

Materials

Diethylenetriamine, *N*,*N*′-methylenebisacrylamide and acrylyl chloride were obtained from Sinopharm Group Chemical Reagent Co., Ltd (China). Cystamine dihydrochloride was obtained from Changzhou Furong Chemical Co., Ltd (China). 2-Hydroxyethyl methacrylate (HEMA), 2,2-dimethoxypropane, glycidyl methacrylate (GMA), dithioerythritol (DTT) and 3-(4, 5-dimethylthiazol-2-yl)-2,5-diphenyl tetrazolium bromide (MTT) were obtained from Shanghai Aladdin Reagent Co., Ltd (China). PEI 25k and *p*-toluenesulfonic acid (pTSA) were obtained from Sigma-Aldrich St. Louis, MO, (USA). Lipofectamine™ 2000 Transfection Reagent (Lipo2000) was obtained from Thermo Fisher Scientific, Waltham, MA (USA). Paclitaxel was obtained from Nanjing Sike Pharmaceutical Co., Ltd (China). The MCF-7 human breast cancer cell line (MCF-7/S) was obtained from the Cell Bank of Shanghai, Institute of Biochemistry and Cell Biology, Chinese Academy of Sciences (China). The paclitaxel-resistant MCF-7 cell line was established as previously described.[3] Negative control siRNA (siN.C. sense strand: 5′-UUC UCC GAA CGU GUC ACG UTT-3′) and TAGLN2 siRNA (sense strand: 5′-CUG AGC GCU AUG GCA UUA ATT-3′) were obtained from GenePharm Co., Ltd (China).

Synthesis of *N*,*N*′-cystamine bisacrylamide

CBA was synthesized through an amidation reaction between cystamine dihydrochloride and acrylyl chloride.[36] Cystamine dihydrochloride (5.8 g, 25 mmol) was added into a 250 mL three-necked flask with 50 mL deionized water in it. An aqueous solution of NaOH (10 mL, 10 mol L^{-1}) and a solution of acrylyl chloride (4.7 g, 50 mmol) in dichloromethane (DCM, 5 mL) were added dropwise under stirring at 0–5 °C. After 1 h of addition, the mixture was stirred at room temperature for 4 h. A white solid product was obtained by filtration. The liquid phase was extracted with DCM 3 times, and the organic extract was dried under Na_2SO_4 overnight. The solvent was removed by rotary evaporation. The final product was obtained as a white solid (3.7 g, yield: 55%) by recrystallization. The chemical structure of CBA was determined using a 600 MHz ^{1}H NMR spectrometer in $CDCl_3$ (shown in the ESI,† Fig. S1).

Synthesis of ketal containing diacrylate

To synthesize KDA, 2,2-dimethoxypropane (2.1 g, 20 mmol), HEMA (5.2 g, 40 mmol) and pTSA (110 mg, 0.64 mmol) were dissolved in dry benzene.[13] The reaction mixture was allowed to stand at 90 °C for 12 h and distilled to remove the methanol–benzene azeotrope. The remaining benzene was removed by rotary evaporation after reaction. The product was purified by

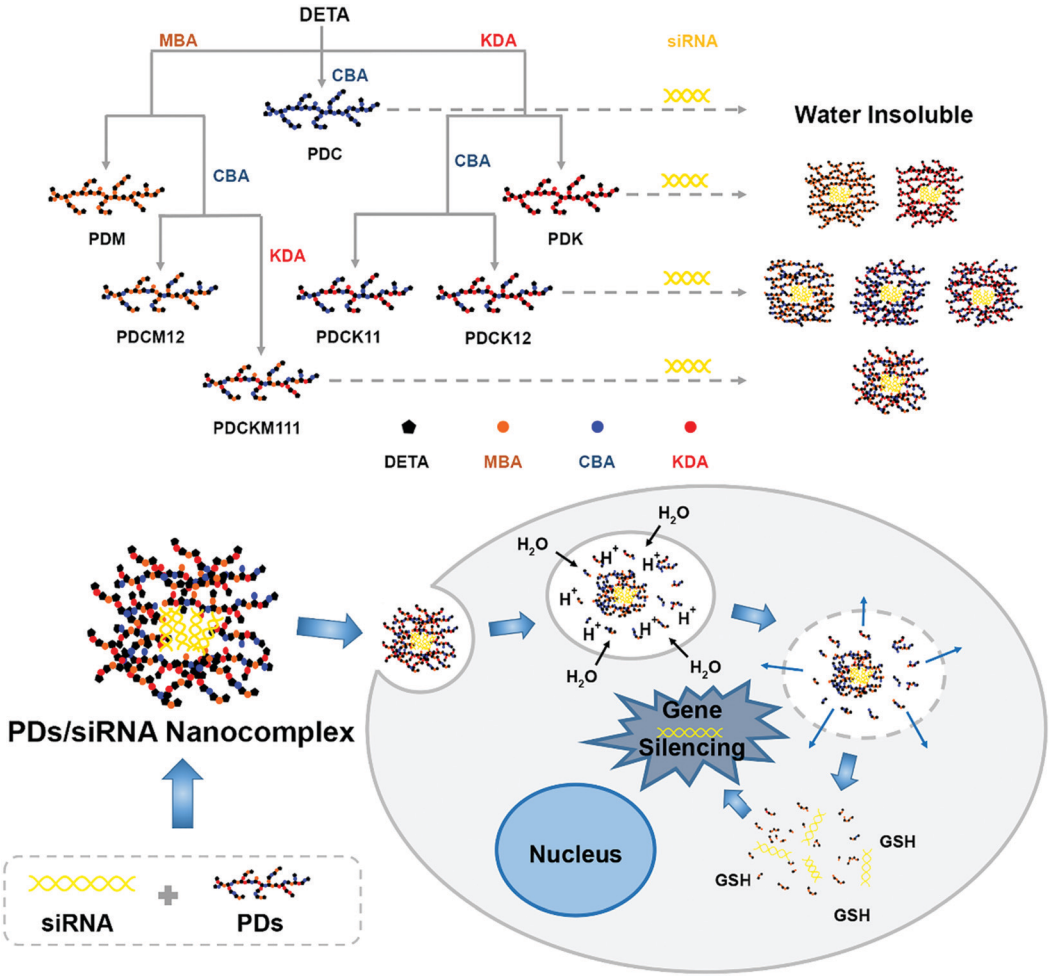

Scheme 1 Schematic diagram illustrating the bound TAGLN2 siRNA and delivery by bioreducible and acid-labile PDs.

column chromatography eluting with 4 : 1 petroleum ether/ethyl acetate and obtained as a colorless liquid (1.2 g, yield: 20%). The chemical structure of KDA was determined using a 600 MHz ^{1}H NMR spectrometer in D_2O (shown in Fig. S2, ESI†).

Synthesis and characterization of PDs

Synthesis of PDs was carried out by the Michael addition reaction between DETA and cross-linkers (MBA, CBA and/or KDA) at 60 °C.[37–41] The reaction conditions and results are shown in Table 1. Typically, to synthesize polydiethylenetriamine with CBA, KDA and MBA (1 : 1 : 1) as cross-linkers (PDCKM), CBA (0.52 g, 2 mmol), KDA (0.60 g, 2 mmol) and MBA (0.31 g, 2 mmol) were added into a solution of DETA (0.62 g, 6 mmol) in a methanol/water mixture (10 mL, 4 : 1, v/v). The reaction was performed at 60 °C in the dark under nitrogen for 4 days. The synthetic process of PDs is shown in Scheme 2. To remove the unreacted monomers, the product was precipitated in an ethyl ether/acetone mixture (1 : 1, v/v) 3 times, and the final product was dissolved in methanol and dried under vacuum for 24 h. The chemical structure of PDs was determined using a 600 MHz ^{1}H NMR spectrometer in $(CD_3)_2SO$ or D_2O. The weight average molecular weight (M_w) and

Table 1 Synthesis conditions and characterization of PDs

	Monomers (equiv.)							
Polymers	CBA	KDA	MBA	DETA	Reaction time (d)	M_w (kDa)	PDI (M_w/M_n)	Lability
PDM	0	0	1	1	2	24.2	1.57	Non
PDC	1	0	0	1	1	—	—	Redox
PDCM12	0.33	0	0.67	1	2	26.3	2.01	Redox
PDK	0	1	0	1	5	12.8	1.8	Acid
PDCK11	0.5	0.5	0	1	2	15.1	1.55	Dual
PDCK12	0.33	0.67	0	1	4	18.8	2.29	Dual
PDCKM	0.33	0.33	0.33	1	4	24.5	2.5	Dual

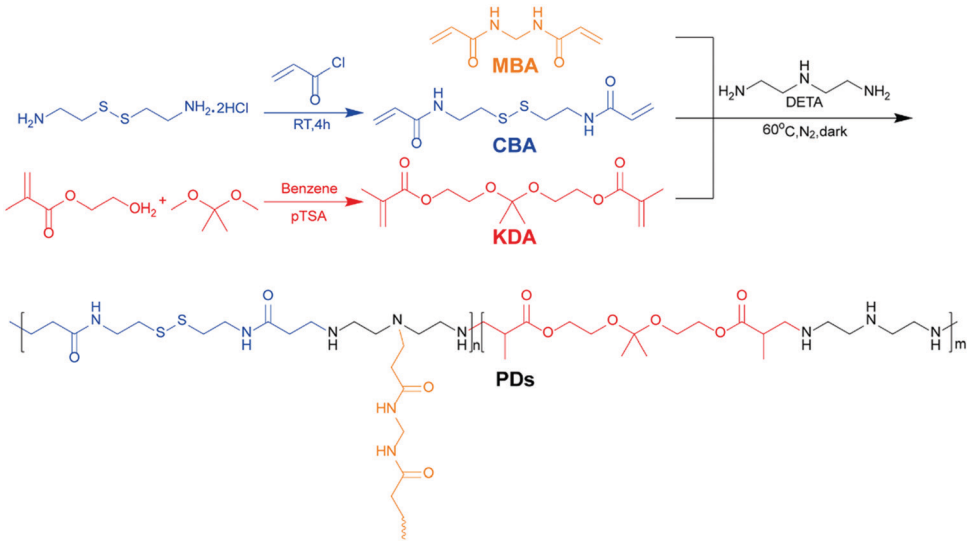

Scheme 2 Synthesis route to CBA, KDA and PDs.

polydispersity (M_w/M_n, PDI) of PDs were measured by gel permeation chromatography (GPC).

Degradation of PDs under different conditions

It has been reported that hyperbranched cationic polymers, such as PAMAM and PAE, can emit visible fluorescence without a fluorescent chromophore.[42–44] And the fluorescence intensity of the hyperbranched cationic polymers was influenced by their molecular weight, and with the increasing polymer M_w the fluorescence intensity enhanced observably.[45,46] Linear and low M_w cationic polymers fluoresce negligibly.[47] In this study, a series of PDs containing different cross-linkers were synthesized at 60 °C, so that hyperbranched polymers can be obtained. Based on this situation, 10 mg mL^{-1} of PDs were incubated under different conditions, and fluorescence was measured using a Fluorescence Spectrophotometer (Shimadzu RF-5301PC, Japan) to analyze the effect of cross-linker proportion on the degradation of PDs. Briefly, PDs (0.1 g) were incubated in 10 mL of pH 7.4 PBS, 10 mM DTT containing pH 7.4 PBS solution or pH 5.0 PBS and measured at different time points, and the decrease of the fluorescence intensity reflects indirectly the degradation under reduction or acidic conditions.[47]

Buffer capacity of PDs

The buffer capacity of PDs was determined by acid–base titration over the pH range from 10.0 to 3.0.[25] Briefly, 10 mg of PDs or PEI 25k was dissolved in 10 mL of 150 mM NaCl solution, and the pH of the sample solution was adjusted to 10.0 with 0.1 M NaOH. The solution was continually titrated with 0.1 M HCl, and the pH value of the solution was measured using an acidometer every 10 μL addition of 0.1 M HCl.

Cytotoxicity assay

The cytotoxicity of PDs was evaluated by MTT assay. MCF-7/S or MCF-7/PTX cells were seeded in a 96-well plate at a density of 1×10^4 cells per well in DMEM containing 10% of FBS and incubated overnight. After this, the cells were treated with various amounts of PDs or PEI 25k for 24 h. The medium was removed, replaced with 200 μL of MTT solution and incubated for another 4 h. Dimethyl sulfoxide (150 μL) was added to dissolve the resulting formazan crystal. The relative viability was measured by quantifying the UV absorbance at 490 nm.

Preparation and characterization of PDs/siRNA nanocomplexes

TAGLN2 siRNA was condensed by PDs to form nanocomplexes through electrostatic interaction in aqueous solution. Briefly, 20 pmol siRNA was dissolved in 20 μL of RNase-free water and added into 80 μL PDs solution. After vortexing for 15 s, the mixture was incubated at room temperature for 30 min.

The formation of nanocomplexes was confirmed by agarose gel retardation assay. Nanocomplex solutions containing 5 pmol siRNA at various N/P ratios were loaded on 1.0% agarose gel in tris-borate-EDTA (TBE) buffer containing 0.5 μg mL^{-1} Dured with loading buffer, electrophoresed for 50 min at 100 V, and visualized under ultraviolet light and photographed using a Gel Doc EZ Imager gel documentation system (Bio-Rad, Hercules, CA, USA).

The particle size and zeta-potential of the nanocomplexes at a siRNA concentration of 200 nM were determined by dynamic light scattering using a Zetasizer Nano ZS90 (Malvern, British).

The morphologies of the nanocomplexes prepared at an N/P ratio of 30 : 1 were observed by transmission electron microscopy (TEM). 2 μL of nanocomplex solution was dropped on a carbon-coated copper grid, and observed under a JEM-2100Plus Transmission Electron Microscope (JEOL, Japan) after 2 h at room temperature.

In vitro dissociation of nanocomplexes

To investigate the acid-lability, nanocomplexes were prepared and incubated at pH 5.0 or pH 7.4 for 4 h and agarose gel electrophoresis was performed. At the same time, 10 mM DTT solution was used to study the dissociation ability of the

nanocomplexes in the reducing environment, and after incubating for 0.5 h, the solution was subjected to agarose gel electrophoresis.

Cellular uptake experiment

MCF-7/PTX cells were seeded into a 24-well plate at a density of 1×10^5 cells per well in DMEM containing 10% of FBS and incubated overnight. Negative control FAM siRNA was used to form FAM-labeled nanocomplexes. The nanocomplex solution was diluted with a serum-free medium and added into the cells at a siRNA concentration of 100 nM. After incubating for 6 h, the cells were washed 3 times with PBS, and 0.4% of trypan blue solution was added to quench the fluorescence outside the cells. After incubating with trypan blue for 3 minutes, the cells were washed 3 times with PBS and visualized under a fluorescence microscope (Olympus, Japan) to observe the transfection efficiency.

Gene silencing *in vitro*

To evaluate the siRNA-mediated gene silencing efficiency, the level of TAGLN2 mRNA transcription and the expression of the TAGLN2 protein were determined by the real-time polymerase chain reaction (RT-PCR) and Western blot analysis. Briefly, MCF-7/PTX cells were seeded into a 6-well plate at a density of 5×10^5 cells per well in DMEM containing 10% of FBS and incubated overnight. TAGLN2 siRNA was used to form nanocomplexes. The nanocomplex solution was diluted with a serum-free medium and added into the cells at a siRNA concentration of 100 nM. After incubating for 6 h, cells were washed 3 times with PBS. The medium was removed, replaced with 2 mL of serum-containing medium and incubated for another 48 h. TAGLN2 RNA and the protein were extracted and gene silencing efficiency was analyzed by RT-PCR and Western blotting.

Influence of nanocomplexes on the cytotoxicity of paclitaxel

MCF-7/PTX cells were seeded into a 96-well plate at a density of 5×10^3 cells per well in DMEM containing 10% of FBS and incubated overnight. TAGLN2 siRNA nanocomplexes, negative control siRNA nanocomplexes or deionized water was diluted with a serum-free medium and added into the cells at a siRNA concentration of 100 nM. After incubating for 6 h, cells were washed 3 times with PBS. The medium was removed, replaced with 200 μL of serum-containing medium and incubated for another 24 h. Then the medium was replaced with various amounts of paclitaxel in serum-containing medium. After 48 h, the relative viability of MCF-7/PTX cells was measured by MTT assay as described above.

Statistical analysis

The data were presented as mean ± standard deviation (SD) and Student's *t*-test was used to analyze the significance of difference between experimental groups. All statistical analyses were performed using SPSS 23.0 and the level of significance was set as $^{**}P < 0.01$.

Results and discussion

Synthesis and characterization of PDs

In this study, MBA, CBA and KDA were chosen as cross-linkers because their α,β-unsaturated carbonyl group can lead to the occurrence of the grafting and crosslinking reactions with DETA. When the reaction temperature was 45 °C, linear polymers will be synthesized, and when the temperature was over 55 °C, hyperbranched polymers can be prepared. In previous studies, the hyperbranched polymer was found to have a higher positive charge density and gene condensing capability, so that 60 °C was chosen to prepare various PDs in this study. PDs with varying degrees of bioreducibility and acid degradability were synthesized *via* the Michael addition reaction by controlling the feed ratios of CBA, MBA and KDA as cross-linkers in order to achieve better water solubility, intracellular siRNA release and transfection efficiency.

In preliminary work, polydiethylenetriamine with MBA as a cross-linker (PDM) and polydiethylenetriamine with CBA as a cross-linker (PDC) were synthesized, but PDC was found to be insoluble in water. According to previous reports,[48–50] such a phenomenon was caused by the cross-linking reaction of excess disulfide bonds in CBA, and water insolubility restricts the applications in gene delivery. In order to prepare bioreducible PDs with better water solubility, the feed ratios of CBA and MBA were changed and PDs with CBA and MBA (1 : 1, 1 : 2 and 1 : 5) as cross-linkers (PDCM11, PDCM12 and PDCM15) were synthesized. It was found that PDCM12 and PDCM15 were water-soluble and PDCM11 was water-insoluble. To examine the reducing degradation ability influenced by the CBA proportion, PDs with CBA and GMA (0 : 1, 1 : 1, 1 : 2 and 1 : 5) as cross-linkers (PDG, PDCG11, PDCG12 and PDCG15) were synthesized (shown in Fig. S3, ESI†). GMA and MBA can react with the amino group of DETA through epoxy and α,β-unsaturated carbonyl groups, and the structures of PDG and PDM are similar to those of hyperbranched polymers at a reaction temperature of 60 °C. And because of the generation of hydroxyl on the molecular chain, all the PDs were found to have good water solubility. To investigate the reducing degradation ability, water soluble PDs were incubated in pH 7.4 PBS or 10 mM DTT PBS solution for 0.5 or 24 h, and the fluorescence intensity was measured to reflect the reducing degradation activity of PDs.[51–53] The result is shown in Fig. S4 (ESI†), and it was found that the fluorescence intensity of PDCM12, PDCG11 and PDCG12 decreased significantly in 0.5 h and maintained in 24 h, which implied their complete degradation in 0.5 h in a reducing environment. The fluorescence intensity of PDCM15 and PDCG15 decreased in 0.5 h, and further decreased in 24 h, and such a result indicated that PDCM15 and PDCG15 will not completely degrade in 0.5 h in a reducing environment. In addition, PDM and PDG showed no obvious degradation in a reducing environment. The results indicated that bioreducible PDs with a ratio of CBA to MBA of 1 : 2 exhibit good water solubility and rapid reducing degradation.

Then, acid-labile KDA was introduced as a cross-linker to obtain bioreducible and/or acid-labile PDK, PDCK11, PDCK12 and PDCKM. It was found that all these PDs including PDCK11

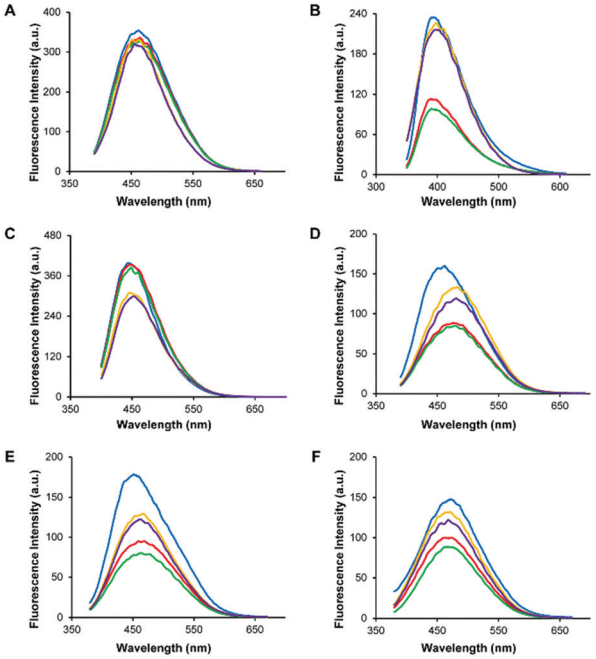

Fig. 1 Emission spectra of (A) PDM excited at 360 nm, (B) PDCM12 excited at 320 nm, (C) PDK excited at 370 nm, (D) PDCK11 excited at 360 nm, (E) PDCK12 excited at 350 nm and (F) PDCKM excited at 350 nm; PDs were incubated with pH 7.4 PBS (blue line), 10 mM DTT 0.5 h (red line), 10 mM DTT 24 h (green line), pH 5.0 PBS 4 h (yellow line) and pH 5.0 PBS 24 h (purple line).

are water soluble, and such a phenomenon may be caused by the formation of hydrogen bonds between ketal bonds and water, so that they would be suitable for siRNA delivery. As shown in Fig. 1, reducing and acid degradation activities of the PDs were measured, and it was found that PDCM12, PDCK11, PDCK12 and PDCKM can be degraded in a reducing environment because of the presence of CBA, and PDK, PDCK11, PDCK12 and PDCKM can be degraded in an acid environment because of the KDA in them. As the portion of KDA increased, PDK and PDCK12 completely degraded, and PDCK11 and PDCKM partially degraded in 4 hours in the acidic environment.

The structure of PDs was confirmed by ^{1}H NMR, shown in Fig. 2, and the disappearance of the proton peaks between 5.0 ppm and 6.5 ppm in the final PDs indicates the complete conversion of the double bonds of acrylamide and acrylate groups. And it was found that the ratio of MBA to CBA and KDA in the final PDs was close to the feed ratio, by the integral ratio of methylene protons of MBA at 4.51 ppm to methylene protons adjacent to the amide groups of CBA at 3.47 ppm and methyl protons of KDA at 1.39 ppm. As a result, PDs with different bioreducibility and acid degradability were synthesized by controlling the feed ratio of the cross-linkers. The M_w and PDI of the PDs were in the range of 12.8 to 26.3 kDa and 1.57 to 2.50 (shown in Table 1).

Buffer capacity of PDs

Buffer capacity is an important property of PDs, and it depends to a certain extent on the positive charge density of PDs. To confirm the buffering capacity of PDs, acid–base titration was carried out, and NaCl and PEI 25k solution were used as control groups. As shown in Fig. 3A, the pH of the NaCl solution rapidly decreased with the addition of HCl solution, suggesting low buffering capacity. However, cationic polymers showed a slow and sustained pH reduction with the addition of HCl solution because of the protonation of the amine groups in the backbone of PDs. PEI 25k showed the best buffering capacity because of its highest positive charge density. Among PD groups, PDM and PDCM12 showed the best buffering capacity, while PDK showed the worst buffering capacity, indicates the different positive charge density of PDs. The low positive charge

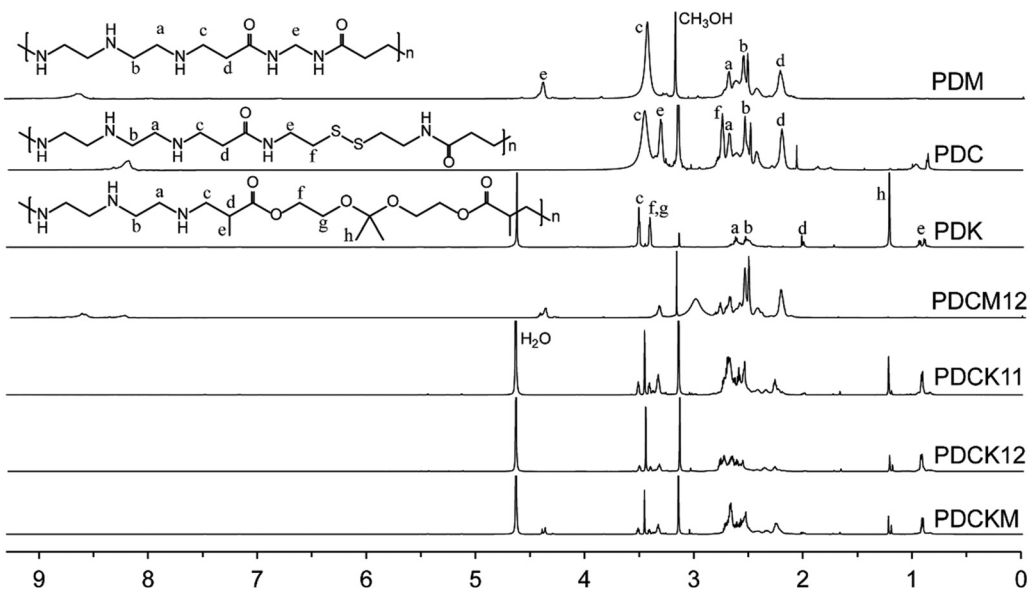

Fig. 2 ^{1}H-NMR spectra (600 MHz) of PDM, PDC and PDCM12 in $(CD_3)_2SO$; PDK, PDCK11, PDCK12 and PDCKM in D_2O.

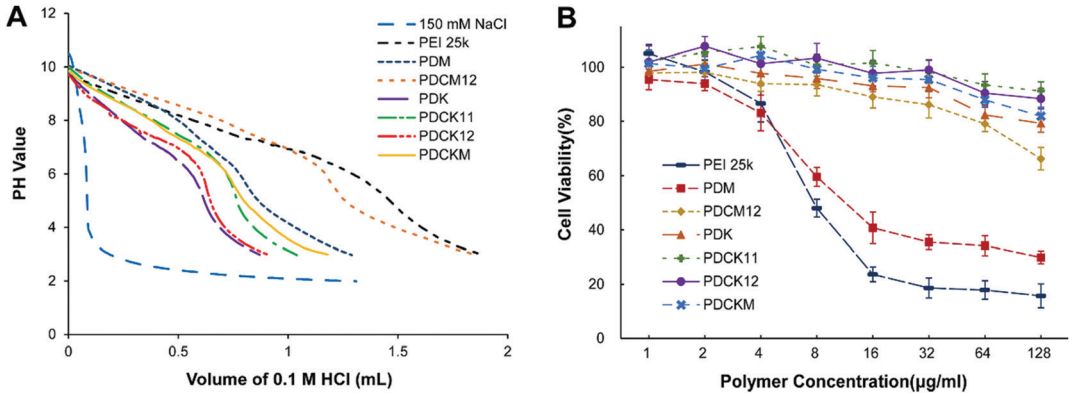

Fig. 3 (A) Titration curves of PDs and PEI in 150 mM NaCl aqueous solution with 0.1 M HCl. (B) Cytotoxicity of PDs and PEI in MCF-7/PTX cells evaluated by the MTT assay. The values are the mean ± SD (n = 6). The incubation time was 24 h with a cell seeding density of 1×10^4 cells per well.

density of PDs may influence the gene binding and the cellular uptake of nanocomplexes. This phenomenon was perhaps due to the methyl groups in KDA, which hampered the polymerization between the acrylate groups of KDA and the amino groups of DETA, so that PDK had the smallest M_w and the worst buffering capacity. It has been reported that, the better buffering capacity of PDs may facilitate endosomal escape of nanocomplexes by the proton sponge effect.[54]

In vitro cytotoxicity of PDs

Cytotoxicity is a hot spot involving the development of siRNA carriers, and it is closely related to the biocompatibility of siRNA delivery systems. In this study, *in vitro* cytotoxicity of PDs was evaluated using the MTT assay. Two different cells (MCF-7/S and MCF-7/PTX cells) were treated with various amounts of PDs for 24 h (shown in Fig. 3B and Fig. S5, ESI†). In comparison to PEI 25k, 32 μg mL^{-1} of PEI 25k caused more than 80% reduction in viability of both two cells. PDM, at a dose of 32 μg mL^{-1}, showed almost 60% reduction in viability of both two cells because of its undegradability. However, the viability of the two cells was not greatly influenced by other PDs, at a dose up to 128 μg mL^{-1} of PDCM12, the viability remained 66.3% in MCF-7/PTX cells and 62.0% in MCF-7/S cells, and dual-responsive PDs showed even lower cytotoxicity, demonstrating the excellent biocompatibility of PDs as a siRNA carrier.

Preparation and characterization of PDs/siRNA nanocomplexes

It is necessary to compact siRNA into stable nanocomplexes for efficient delivery. Gel retardation assay was performed to evaluate the siRNA condensing capability of PDs at different N/P ratios from 1 : 1 to 15 : 1. As shown in Fig. 4, PEI 25k showed the best siRNA condensing capability, and the siRNA band disappeared at an N/P ratio of 10 : 1. Total retardation of nanocomplexes was observed for PDM, PDCM12 and PDCKM at an N/P ratio of 10, but for PDK, PDCK11 and PDCK12 it was 15 : 1, which indicated that PDs with less KDA showed a higher positive charge density and exhibited enhanced capability to

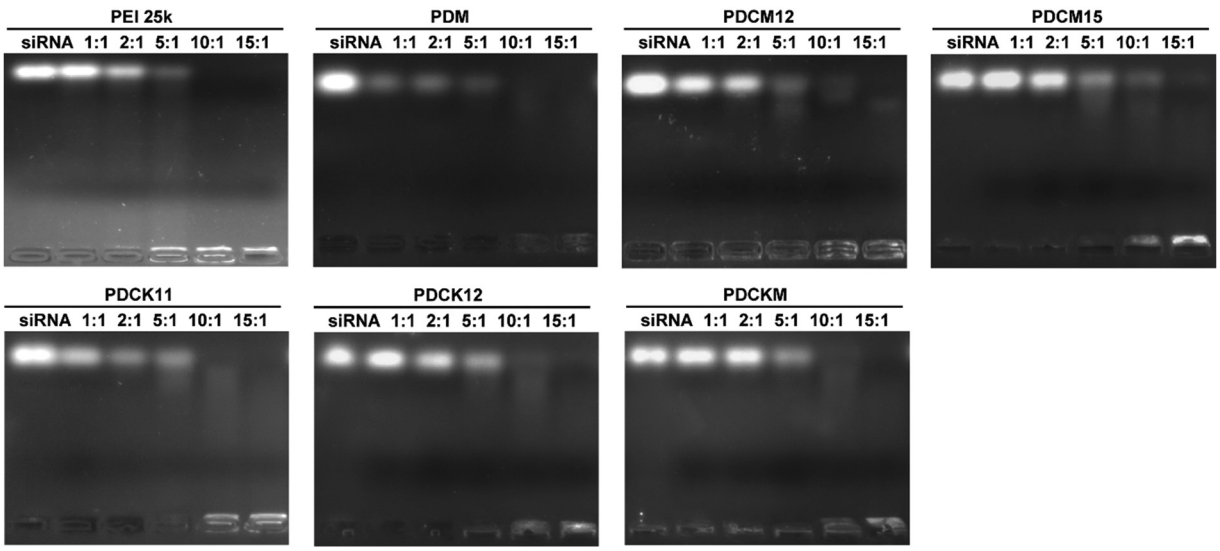

Fig. 4 Agarose gel electrophoresis of PDs/siRNA and PEI/siRNA nanocomplexes at various N/P ratios. The nanocomplexes were incubated in pH 7.4 PBS to investigate the siRNA binding capacity.

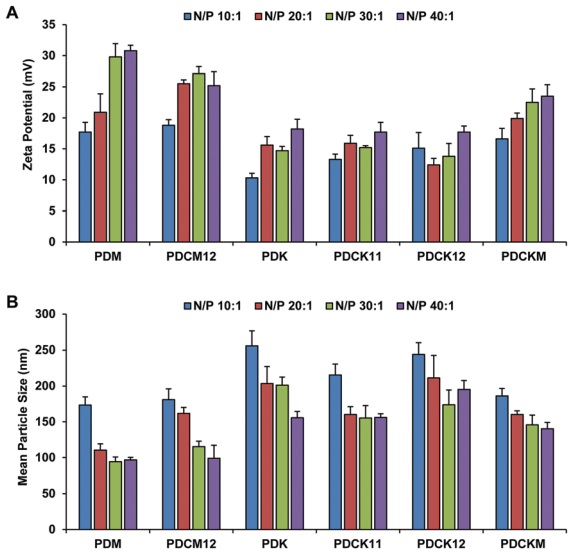

Fig. 5 (A) Zeta potential and (B) mean particle sizes of various PDs/siRNA nanocomplexes at different N/P ratios. The values are mean ± SD (n = 3).

condense siRNA. This result matched the buffering capability of PDs measured before.

Fig. 5A shows the particle sizes of nanocomplexes measured by dynamic light scattering, and PDs could condense siRNA into nanocomplexes with a small particle size (90–200 nm) at an N/P ratio of 40 : 1. With the increase of the N/P ratio from 10 : 1 to 30 : 1, almost all the particle sizes decreased, and this phenomenon was deemed to condense siRNA by PDs. However, when the N/P ratio was up to 40 : 1, the particle sizes changed negligibly, indicating the complete condensation of siRNA, so that the N/P ratio was set at 30 : 1 for further research. PDM had the smallest particle size (94.4 nm) at an N/P ratio of 30 : 1 because of the high positive charge density and preferable siRNA condensation capability. As shown in Fig. 5B, the surface charge of the nanocomplexes increased with the increase of the N/P ratio, and all PDs formed nanocomplexes had a positive charge at an N/P ratio of 10 : 1. However, the zeta potentials of PDK, PDCK11 and PDCK12 were lower, and a possible reason is that the ether group in KDA and the lower Mw may influence the positive charges of these PDs.

Fig. 6 shows the morphologies of various nanocomplexes observed by TEM. The morphologies of nanocomplexes condensed by PDM, PDCM12 and PDCKM appeared as more compact spheres with smaller sizes (100–150 nm) than PDK, PDCK11 and PDCK12. As expected from the zeta potential (Fig. 5A) and mean particle sizes (Fig. 5B), PDM, PDCM12 and PDCKM have a higher positive charge density so that they can condense siRNA into more compact spheres. With the increase of the KDA proportion, PDCK11, PDCK12 and PDK showed a lower positive charge density resulting in more loosened morphologies and bigger sizes.

In vitro dissociation of nanocomplexes

To investigate the dissociation of nanocomplexes under reduction or acidic conditions, siRNA/PDs nanocomplexes at an N/P ratio of 30 were incubated under different conditions, and the results were demonstrated by agarose gel electrophoresis (shown in Fig. 8A). No detectable dissociation was observed at a pH of 7.4 even over 4 hours in all PDs, indicating the excellent stability of nanocomplexes. When incubated in PBS at a pH of 5.0, siRNA was completely released from PDK and PDCK12, partly released from PDCK11, and slightly released from PDCKM. When incubated with 10 mM DTT for 30 minutes, siRNA was released from the nanocomplexes of PDCM12, PDCK11, PDCK12 and PDCKM. By forming interchain disulfide bonds, nanocomplexes could be readily cross-linked into a stable structure, and the rapid degradation of

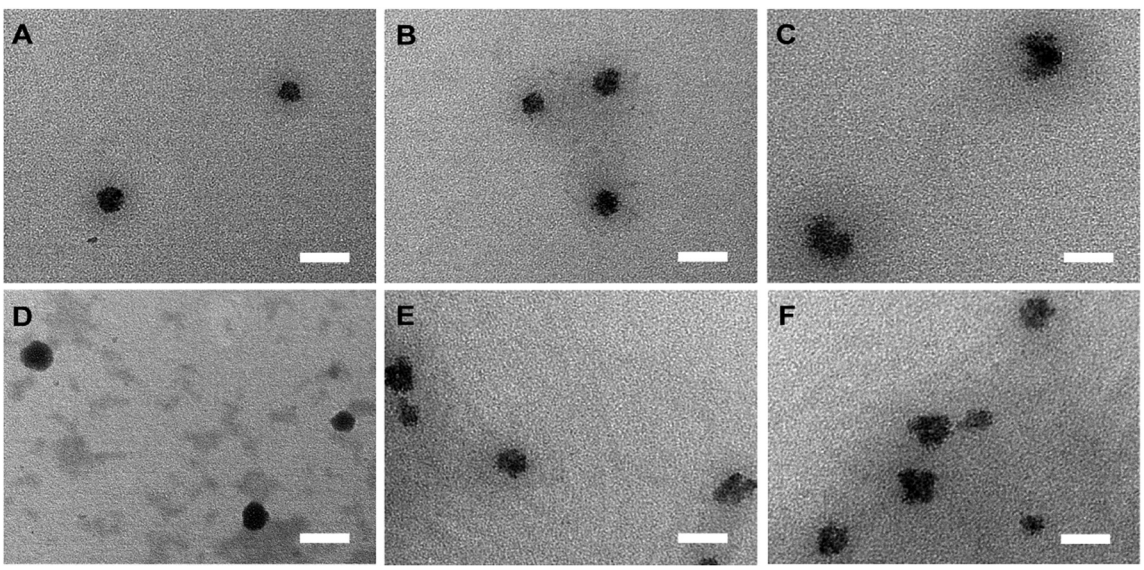

Fig. 6 Representative TEM micrographs of nanocomplexes condensed by (A) PDM, (B) PDCM12, (C) PDK, (D) PDCKM, (E) PDCK11 and (F) PDCK12 at 30 : 1 N/P ratio. Scale bar = 200 nm.

nanocomplexes in DTT solution was caused by the breaking of the disulfide bonds. It was hypothesized that at pH 5.0 PDK and PDCK12 degraded into small residues, which were unable to interact with siRNA, resulting in the release of siRNA from nanocomplexes. The premature release of siRNA into an acidic environment, such as that of the endosome, can lead to degradation of siRNA. However, siRNA would be partially released from the nanocomplexes of PDCK11 and PDCKM at pH 5.0, because these PDs partially degraded into low M_w polymers in the acidic environment, but this cleavage was not strong enough to release siRNA rapidly. This characteristic may actually improve the transfection efficiency of PDs, because the small molecular product will increase the osmotic pressure in endosomes, leading to endosomal disruption. The optimum content of ketal bonds in PDs could facilitate endosomal escape without too much siRNA release. This speculation was confirmed in the subsequent transfection study.

Cellular uptake of nanocomplexes

The cellular uptake of nanocomplexes was performed using siRNA labeled with FAM on MCF-7/PTX cells. FAM was used as an intercalating dye with high affinity to siRNA. MCF-7/PTX cells were incubated with nanocomplexes containing FAM-labeled siRNA for 6 h, and Fig. 7 shows the cellular uptake of nanocomplexes, and the green fluorescence of FAM-siRNA in the cytoplasm gradually increased with the decrease of the KDA proportion. There was little fluorescence detected in PDK and PDCK12 treated cells, while fluorescence was distributed in the cytoplasmic compartment of PDCK11 and PDCKM treated cells. Fluorescence in PDM and PDCM12 treated cells was comparable to that of PEI. There are some probable reasons for this phenomenon, PDK and PDCK12 nanocomplexes showed a lower positive charge density, which may influence the uptake of nanocomplexes, the acidic environment of tumor cells may induce the siRNA release before cellular uptake, the premature release of siRNA in endosomes may cause substantial siRNA hydrolysis and the fluorescence of FAM may be quenched in the acidic environment without protection of PDs.

Silencing efficiency of TAGLN2 *in vitro*

To evaluate the siRNA-mediated gene silencing efficiency of PDs, the levels of mRNA transcription and protein expression were determined by RT-PCR and Western blot analysis, respectively (shown in Fig. 8B and C). Fig. 8B shows the expression of TAGLN2 mRNA, and compared with other formulations, PDCKM showed the highest silencing efficiency of 52.98% mRNA down-regulation in MCF-7/PTX cells, which validated that the enhanced cellular uptake and efficient intracellular release of siRNA resulted in the elevated gene-silencing efficiency. In line with this, at the protein expression level, TAGLN2 siRNA delivered by PDCKM remarkably down-regulated the expression of the TAGLN2 protein in MCF-7/PTX cells even better than PEI 25k and Lipo2000 (Fig. 8C). This may be due to the good water solubility, enough positive charge density, rapid reducing degradation and endosomal escape without siRNA releasing PDCKM. At the same time, the differences between naked siRNA, PDCKM/siN.C. and the control group were not significant. This phenomenon indicated that the down-regulation of TAGLN2 mainly happened after TAGLN2 siRNA was released into the cytoplasm.

Influence of nanocomplexes on the cytotoxicity of paclitaxel

As shown in Fig. 9, TAGLN2 siRNA was condensed by PDCKM at an N/P of 30 : 1, which showed the best silencing efficiency in MCF-7/PTX cells. PBS (pH 7.4) was used as the control agent, and MCF-7/PTX cells incubated with PDCKM/negative siRNA nanocomplexes showed similar cell viability when treated with paclitaxel to control group, because negative siRNA cannot down-regulate the expression of TAGLN2. MCF-7/PTX cells incubated with PDCKM/TAGLN2 siRNA nanocomplexes showed enhanced paclitaxel cytotoxicity, after one-way ANOVA followed by the least significant difference (LSD) test, and the difference of cell viability between TAGLN2 siRNA and the control group ($p < 0.05$) was obvious, which was due to the silencing of TAGLN2 at mRNA and protein levels. The half maximal inhibitory concentration (IC_{50}) of TAGLN2 siRNA, negative siRNA and

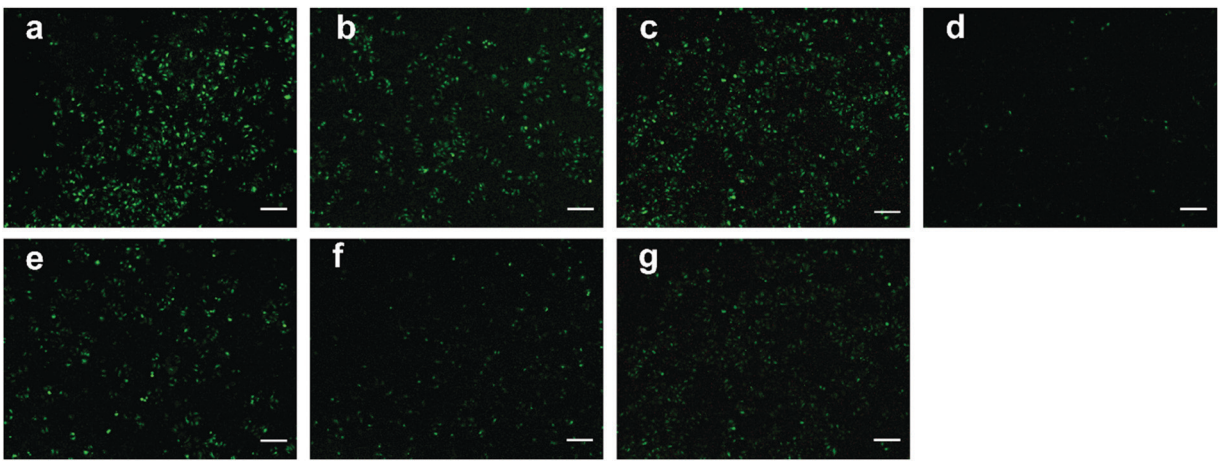

Fig. 7 Cellular uptake of PDs/FAM-siRNA and PEI/FAM-siRNA nanocomplexes in MCF-7/PTX cells. Fluorescence images of cellular uptake of (a) PEI 25k, (b) PDM, (c) PDCM12, (d) PDK, (e) PDCK11, (f) PDCK12 and (g) PDCKM.

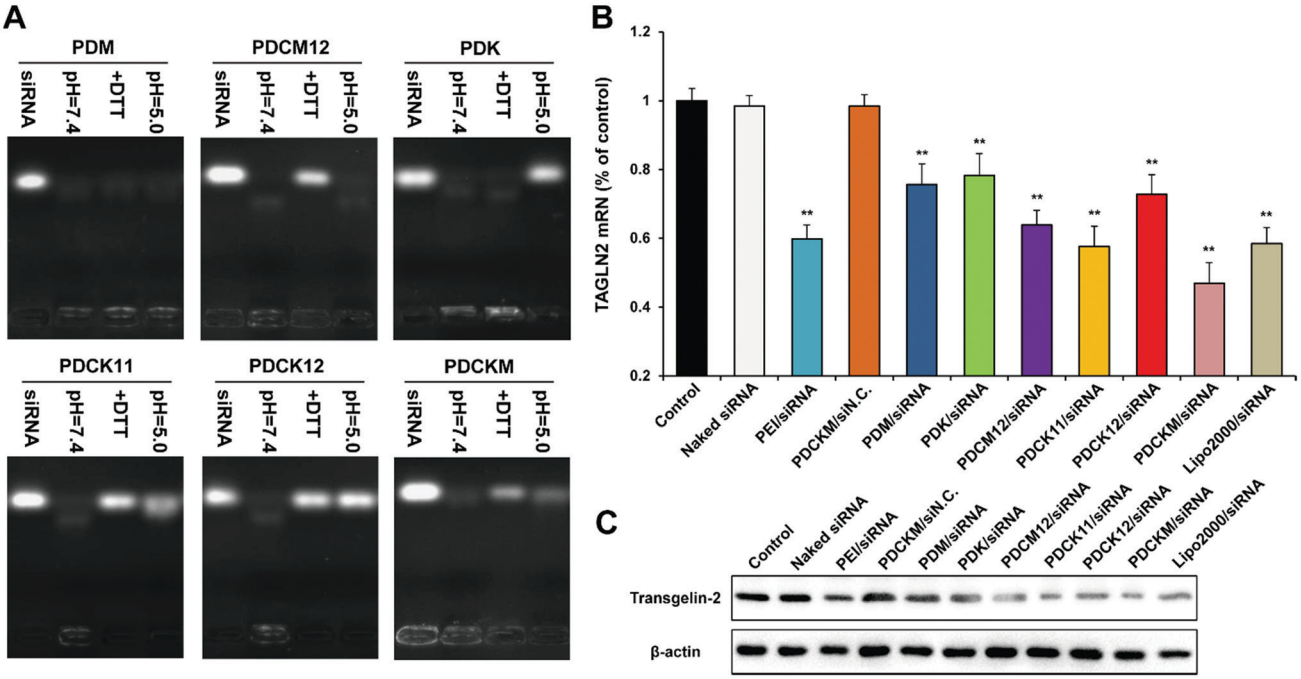

Fig. 8 (A) Agarose gel electrophoresis of PDs/siRNA nanocomplexes at an N/P ratio of 30 : 1. Naked siRNA, nanocomplexes incubated in pH 7.4 PBS for 4 h, nanocomplexes incubated in 10 mM of DTT solution for 0.5 h or nanocomplexes incubated in pH 5.0 PBS for 4 h were subjected to agarose gel electrophoresis to investigate the dissociation of nanocomplexes under different conditions. (B) MCF-7/PTX cells treated with different nanocomplexes to evaluate the siRNA-mediated gene silencing efficiency. The values are mean ± SD (n = 3). TAGLN2 mRNA expression determined by RT-PCR. $^{**}P < 0.01$ relative to the control group. (C) TAGLN2 protein expression determined by Western blot analysis.

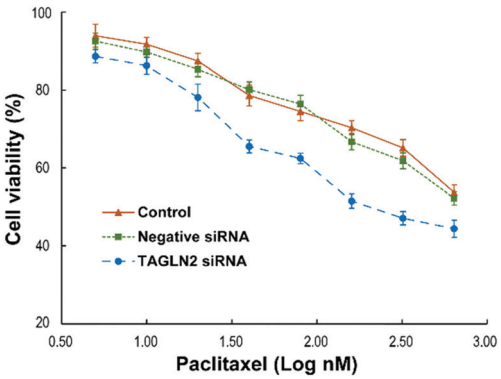

Fig. 9 Cytotoxicity of paclitaxel in MCF-7/PTX cells evaluated by the MTT assay. The values are mean ± SD (n = 6). MCF-7/PTX cells were treated with pH 7.4 PBS, PDCKM/negative siRNA or PDCKM/TAGLN2 siRNA nanocomplexes, and the medium was replaced with various amounts of paclitaxel to evaluate the cell viability.

the control group was 267.5 ± 16.3 nM, 1422.8 ± 73.7 nM and 1574.9 ± 87.5 nM, respectively. The results indicated that TAGLN2 is associated with paclitaxel resistance in MCF-7/PTX cells, and PDs could be used in siRNA delivery to reverse multidrug resistance.

Conclusions

In this study, bioreducible and acid-labile PDs were synthesized for TAGLN2 siRNA delivery. Significant gene transfection ability of this dual-responsive polymer was achieved by sequential degradability, which was higher than that of non-responsive or single-responsive polymers. At the same time, the presence of biodegradable bonds in the polymer resulted in reduction of cytotoxicity in comparison with the non-degradable polymers, including PEI 25k. After treatment with PDs/siRNA nanocomplexes, MCF-7/PTX cells are more susceptible to paclitaxel treatment than untreated cells. Although PDs/siRNA nanocomplexes are easy to disassemble in the systemic circulation, chemical modifications such as PEGylation can be utilized to design novel serum-resistant gene delivery vectors to reverse multidrug resistance in breast cancer. Overall, this novel dual-responsive gene delivery system is an innovative approach for TAGLN2 siRNA delivery, and its sequential degradability enhanced the endosomal escape and cytoplasmic release of siRNA; such properties would be suitable for the delivery of siRNA and it has potential for cancer therapy and multidrug resistance reversal.

Conflicts of interest

The manuscript was written through contributions of all authors. The authors confirm that there are no conflicts to declare.

Acknowledgements

This work was supported financially by the Natural Science Foundation of China (No. 81672954 and 81773663) and the Project of

Independent Innovative Experiment for Postgraduates in medicine in Xi'an Jiaotong University (Grant No. YJSCX-2018-008).

References

1 Y. Zong, J. Wu and K. Shen, *Oncotarget*, 2017, **8**, 17360–17372.
2 W. L. Sun, D. Lan, T. Q. Gan and Z. W. Cai, *Neoplasma*, 2015, **62**, 199–208.
3 J. Cai, S. Chen, W. Zhang, S. Hu, J. Lu, J. Xing and Y. Dong, *Phytomedicine*, 2014, **21**, 984–991.
4 S. Chen, Q. Dong, S. Hu, J. Cai, W. Zhang, J. Sun, T. Wang, J. Xie, H. He, J. Xing, J. Lu and Y. Dong, *Mol. BioSyst.*, 2014, **10**, 294–303.
5 J. Cai, S. Chen, W. Zhang, X. Zheng, S. Hu, C. Pang, J. Lu, J. Xing and Y. Dong, *Phytomedicine*, 2014, **21**, 1725–1732.
6 X. Zheng, S. Chen, Q. Yang, J. Cai, W. Zhang, H. You, J. Xing and Y. Dong, *Cancer Biol. Ther.*, 2015, **16**, 1407–1414.
7 Y. Lai, X. Xu, Z. Zhu and Z. Hua, *Int. J. Nanomed.*, 2018, **13**, 6603–6623.
8 M. K. Riley and W. Vermerris, *Nanomaterials*, 2017, **7**(5), 94.
9 E. H. Jeong, H. Kim, B. Jang, H. Cho, J. Ryu, B. Kim, Y. Park, J. Kim, J. B. Lee and H. Lee, *Adv. Drug Delivery Rev.*, 2016, **104**, 29–43.
10 Y. Dai and X. Zhang, *Macromol. Biosci.*, 2019, e1800445, DOI: 10.1002/mabi.201800445.
11 B. Thapa, S. Plianwong, K. C. Remant Bahadur, B. Rutherford and H. Uludag, *Acta Biomater.*, 2016, **33**, 213–224.
12 J. Li, H. Liang, J. Liu and Z. Wang, *Int. J. Pharm.*, 2018, **546**, 215–225.
13 K. Guk, H. Lim, B. Kim, M. Hong, G. Khang and D. Lee, *Int. J. Pharm.*, 2013, **453**, 541–550.
14 K. L. Kozielski, S. Y. Tzeng and J. J. Green, *Chem. Commun.*, 2013, **49**, 5319–5321.
15 A. E. Arnold, P. Czupiel and M. Shoichet, *J. Controlled Release*, 2017, **259**, 3–15.
16 F. Joris, L. De Backer, T. Van de Vyver, C. Bastiancich, S. C. De Smedt and K. Raemdonck, *J. Controlled Release*, 2018, **269**, 266–276.
17 J. Zhu, M. Qiao, Q. Wang, Y. Ye, S. Ba, J. Ma, H. Hu, X. Zhao and D. Chen, *Biomaterials*, 2018, **162**, 47–59.
18 M. Wojnilowicz, A. Glab, A. Bertucci, F. Caruso and F. Cavalieri, *ACS Nano*, 2019, **13**(1), 187–202.
19 D. Fischer, T. Bieber, Y. Li, H. P. Elsasser and T. Kissel, *Pharm. Res.*, 1999, **16**, 1273–1279.
20 W. T. Godbey, K. K. Wu and A. G. Mikos, *J. Biomed. Mater. Res.*, 1999, **45**, 268–275.
21 B. Ozpolat, A. K. Sood and G. Lopez-Berestein, *Adv. Drug Delivery Rev.*, 2014, **66**, 110–116.
22 D. Xia, L. B. Feng, X. L. Wu, G. D. Xia and L. Xu, *Mol. Med. Rep.*, 2015, **12**, 2336–2342.
23 S. Y. Wong, J. M. Pelet and D. Putnam, *Prog. Polym. Sci.*, 2007, **32**, 799–837.
24 P. Pereira, M. Barreira, J. A. Queiroz, F. Veiga, F. Sousa and A. Figueiras, *Expert Opin. Drug Delivery*, 2017, **14**, 353–371.
25 H. Lim, J. Noh, Y. Kim, H. Kim, J. Kim, G. Khang and D. Lee, *Biomacromolecules*, 2013, **14**, 240–247.
26 Z. Q. Yu, J. T. Sun, C. Y. Pan and C. Y. Hong, *Chem. Commun.*, 2012, **48**, 5623–5625.
27 G. Chen, Y. Wang, R. Xie and S. Gong, *J. Controlled Release*, 2017, **259**, 105–114.
28 D. S. Manickam, J. Li, D. A. Putt, Q. H. Zhou, C. Wu, L. H. Lash and D. Oupicky, *J. Controlled Release*, 2010, **141**, 77–84.
29 N. Zheng, Z. Song, Y. Liu, R. Zhang, R. Zhang, C. Yao, F. M. Uckun, L. Yin and J. Cheng, *J. Controlled Release*, 2015, **205**, 231–239.
30 Y. Y. Peng, D. Diaz-Dussan, P. Kumar and R. Narain, *Biomacromolecules*, 2018, **19**, 4052–4058.
31 N. Leber, L. Kaps, M. Aslam, J. Schupp, A. Brose, D. Schaffel, K. Fischer, M. Diken, D. Strand, K. Koynov, A. Tuettenberg, L. Nuhn, R. Zentel and D. Schuppan, *J. Controlled Release*, 2017, **248**, 10–23.
32 T. Wang, S. Shigdar, H. A. Shamaileh, M. P. Gantier, W. Yin, D. Xiang, L. Wang, S. F. Zhou, Y. Hou, P. Wang, W. Zhang, C. Pu and W. Duan, *Cancer Lett.*, 2017, **387**, 77–83.
33 B. Theek, F. Gremse, S. Kunjachan, S. Fokong, R. Pola, M. Pechar, R. Deckers, G. Storm, J. Ehling, F. Kiessling and T. Lammers, *J. Controlled Release*, 2014, **182**, 83–89.
34 S. S. Kim, J. B. Harford, M. Moghe, A. Rait, K. F. Pirollo and E. H. Chang, *Nucleic Acids Res.*, 2018, **46**, 1424–1440.
35 M. Goldshtein, E. Forti, E. Ruvinov and S. Cohen, *Int. J. Pharm.*, 2016, **515**, 46–56.
36 W. Yang and C. Y. Pan, *Macromol. Rapid Commun.*, 2009, **30**, 2096–2101.
37 L. Xie, X. Ding, R. Budry and G. Mao, *Int. J. Nanomed.*, 2018, **13**, 4943–4960.
38 W. Cheng, D. Wu and Y. Liu, *Biomacromolecules*, 2016, **17**, 3115–3126.
39 W. Cheng, J. N. Kumar, Y. Zhang and Y. Liu, *Biomater. Sci.*, 2015, **3**, 597–607.
40 Y. Liu, Y. Li, D. Keskin and L. Shi, *Adv. Healthcare Mater.*, 2019, **8**, e1801359.
41 D. Zhou, L. Cutlar, Y. Gao, W. Wang, J. O'Keeffe-Ahern, S. McMahon, B. Duarte, F. Larcher, B. J. Rodriguez, U. Greiser and W. Wang, *Sci. Adv.*, 2016, **2**, e1600102.
42 D. Wang and T. Imae, *J. Am. Chem. Soc.*, 2004, **126**, 13204–13205.
43 X. Miao, T. Liu, C. Zhang, X. Geng, Y. Meng and X. Li, *Phys. Chem. Chem. Phys.*, 2016, **18**, 4295–4299.
44 W. I. Lee, Y. Bae and A. J. Bard, *J. Am. Chem. Soc.*, 2004, **126**, 8358–8359.
45 L. Ye and S. H. Goh, *Macromolecules*, 2005, **38**, 9906–9909.
46 Y. Zhang, W. Huang, Y. Zhou and D. Yan, *Chem. Commun.*, 2007, 2587–2589, DOI: 10.1039/b701043e.
47 W. Yang, C. Y. Pan, X. Q. Liu and J. Wang, *Biomacromolecules*, 2011, **12**, 1523–1531.
48 Z. K. Wang, L. H. Wang, J. T. Sun, L. F. Han and C. Y. Hong, *Polym. Chem.*, 2013, **4**, 1694–1699.
49 D. Bermejo-Velasco, A. Azemar, O. P. Oommen, J. Hilborn and O. P. Varghese, *Biomacromolecules*, 2019, **20**, 1412–1420.

50 M. Mackiewicz, J. Romanski, E. Drozd, B. Gruber-Bzura, P. Fiedor, Z. Stojek and M. Karbarz, *Int. J. Pharm.*, 2017, **523**, 336–342.
51 J. Yang, Y. Zhang, S. Gautam, L. Liu, J. Dey, W. Chen, R. P. Mason, C. A. Serrano, K. A. Schug and L. Tang, *Proc. Natl. Acad. Sci. U. S. A.*, 2009, **106**, 10086–10091.
52 X. Chen, H. Yang, C. Xiao and X. Chen, *Macromol. Biosci.*, 2019, **19**, e1800438.
53 W. Yang, C. Y. Pan, M. D. Luo and H. B. Zhang, *Biomacromolecules*, 2010, **11**, 1840–1846.
54 B. Singh, S. Maharjan, T. E. Park, T. Jiang, S. K. Kang, Y. J. Choi and C. S. Cho, *Macromol. Biosci.*, 2015, **15**, 622–635.